



# Salinity stress changed the biogeochemical controls on CH<sub>4</sub> and N<sub>2</sub>O emissions of estuarine and intertidal sediments

Xiaofei Li <sup>a,b,\*</sup>, Dengzhou Gao <sup>c</sup>, Lijun Hou <sup>d</sup>, Min Liu <sup>c</sup>

<sup>a</sup> Key Laboratory for Humid Subtropical Eco-geographical Processes of the Ministry of Education, Fujian Normal University, Fuzhou 350007, China

<sup>b</sup> School of Geographical Sciences, Fujian Normal University, Fuzhou 350007, China

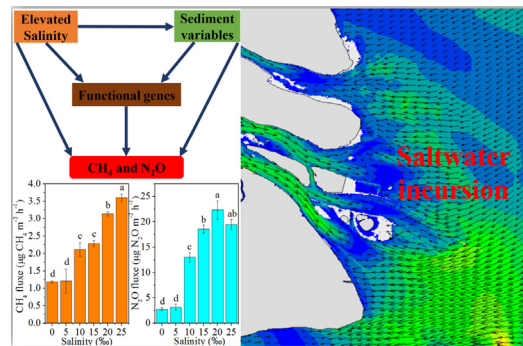
<sup>c</sup> Key Laboratory of Geographic Information Science of the Ministry of Education, School of Geographic Sciences, East China Normal University, Shanghai, 200241, China

<sup>d</sup> State Key Laboratory of Estuarine and Coastal Research, East China Normal University, Shanghai, 200062, China

## HIGHLIGHTS

- Sediment properties were strongly affected by the elevated salinity.
- Labile organic carbon dominated significantly the CH<sub>4</sub> emission rate.
- Denitrification was the determinant of N<sub>2</sub>O emission under increasing salinity.
- Elevated salinity could lead to increased carbon and nitrogen export.

## GRAPHICAL ABSTRACT



## ARTICLE INFO

### Article history:

Received 6 September 2018

Received in revised form 21 October 2018

Accepted 22 October 2018

Available online 22 October 2018

Editor: Shuzhen Zhang

### Keywords:

Biogeochemical controls  
Extracellular enzyme activity  
CH<sub>4</sub> and N<sub>2</sub>O  
Functional gene  
Saltwater incursion

## ABSTRACT

Elevated salinity is expected to drive changes in biogeochemical cycling and microbial communities in estuarine and intertidal wetlands. However, limited information regarding the role of salinity in shaping biogeochemical controls and mediating greenhouse gas emissions is currently available. In this study, we used incubation experiment across salinity gradients of the estuarine and intertidal sediments to reveal the underlying interconnections of CH<sub>4</sub> and N<sub>2</sub>O emissions, biogeochemical controls and salinity gradients. Our results indicated that sediment biogeochemical properties were significantly affected by the increasing salinity, which were attributed to the accelerated sediment enzyme activities. The increasing salinity promoted CH<sub>4</sub> and N<sub>2</sub>O emission rates by stimulating organic carbon decomposition and nitrogen transformation rates. In addition, the copy number of *mcrA*, *nirS* and *nirK* genes increased along with the salinity gradients, which strongly mediated the CH<sub>4</sub> and N<sub>2</sub>O emission rates. Stepwise regression analysis suggested that labile organic carbon and denitrification were the most crucial determinants of CH<sub>4</sub> and N<sub>2</sub>O emission rates, respectively. Overall, salinity could enhance CH<sub>4</sub> and N<sub>2</sub>O emission mainly by altering sediment geochemical variables, microbial activity and functional gene abundance in estuarine and intertidal environments. Furthermore, increasing salinity could enhance the carbon and nitrogen export, which may pose a threat to the ecological function of estuarine and intertidal ecosystems. This study may contribute to the knowledge about the importance of biogeochemical controls induced by salinity in mediating greenhouse gas emissions.

© 2018 Elsevier B.V. All rights reserved.

\* Corresponding author at: Key Laboratory for Humid Subtropical Eco-geographical Processes of the Ministry of Education, Fujian Normal University, Fuzhou 350007, China.  
E-mail address: [lixiaofei198702@126.com](mailto:lixiaofei198702@126.com) (X. Li).

## 1. Introduction

Saltwater incursion into freshwater ecosystems induced by sea level rise under climate change has recently increased in some parts of the world (Wigley, 2005; Church and White, 2006; Morrissey et al., 2014), thus altering microbial metabolism and biogeochemical cycling (Weston et al., 2011; Neubauer et al., 2013; Morrissey et al., 2014). In particular, elevated salinity has been shown to accelerate microbial enzymatic hydrolysis (Weston et al., 2011; Morrissey et al., 2014), which mediates microbial decomposition rates and organic carbon accumulation in tidal wetlands (Craft, 2007; Loomis and Craft, 2010; Morrissey et al., 2014). Microbially mediated nitrogen transformation processes, such as nitrification and denitrification, are also influenced by salinity changes in estuarine and coastal wetlands (Ardón et al., 2013; Hou et al., 2013; Deng et al., 2015). Likewise, salinity has been reported to be a significant driver shaping microbial community structure, which has been identified in both natural environments (Crump et al., 2004; Morrissey et al., 2014) and experimental incubations (Mandee, 2006). Therefore, increasing concerns have been raised regarding the microbial mechanisms of salinity-induced changes in biogeochemical cycling of estuarine and coastal environments (Craft, 2007; Loomis and Craft, 2010; Weston et al., 2011; Neubauer et al., 2013; Morrissey et al., 2014). It has been suggested that greenhouse gases emissions are highly variable in space, and are mainly attributed to salinity changes under the tidal fluctuations in the estuarine environments (Harley et al., 2015). In addition, estuarine and coastal wetlands are easily subject to the changes of biogeochemical variables induced by salinity (Morrissey et al., 2014), which play important roles in affecting the greenhouse gas emissions (Helton et al., 2014). However, the relative importance of abiotic and biotic controls on regulation of greenhouse gas emissions under the conditions of elevated salinity remains unclear.

Methane (CH<sub>4</sub>) and nitrous oxide (N<sub>2</sub>O) are important greenhouse gases (Randeniya et al., 2002; IPCC, 2014). Over the past decades, CH<sub>4</sub> and N<sub>2</sub>O emissions from aquatic ecosystems have become a popularly discussed environmental issue (Randeniya et al., 2002; IPCC, 2014). Globally, freshwater ecosystems contribute most significant CH<sub>4</sub> and N<sub>2</sub>O concentrations to the atmosphere (Bastviken et al., 2011; Helton et al., 2014), highlighting the necessity of identifying the microbial mechanisms of CH<sub>4</sub> and N<sub>2</sub>O emissions in these environments. Because greenhouse gases are mainly generated by microbial processes, microbial composition and abundance play a primary role in regulating CH<sub>4</sub> and N<sub>2</sub>O emissions (S.Y. Zhao et al., 2018). Tong et al. (2017) have reported that the community structure and abundance of methanogens vary strongly across the freshwater–brackish wetlands, leading to differences in CH<sub>4</sub> emissions in subtropical estuarine marshes. Nitrification contributes to N<sub>2</sub>O emission (Russow et al., 2009; Xu et al., 2014), the ammonia-oxidizing microbe thus has attracted much attention in estuarine environments (Hugoni et al., 2015). Zheng et al. (2014) have revealed that the ammonia-oxidizing communities are dissimilar in estuarine and intertidal sediments, bacterial *amoA* is abundant at low salinity while archaeal *amoA* is abundant at high salinity. The *nirS* and *nirK* in denitrifier communities are the microbial producers of N<sub>2</sub>O, while *nosZ* reduces N<sub>2</sub>O to N<sub>2</sub> (Henry et al., 2006; S.Y. Zhao et al., 2018). However, the denitrifier communities are influenced by salinity changes, which likely demonstrate important influences on N<sub>2</sub>O emissions (Franklin et al., 2017). In addition, it has been reported that extracellular enzyme activities are susceptible to salinity changes (Morrissey et al., 2014), which play a crucial role in carbon and nitrogen cycling (Morrissey et al., 2014; Li et al., 2015) and further mediate CH<sub>4</sub> and N<sub>2</sub>O emissions. Previous studies have reported that sulfate, nitrate and ferric iron, which involve the most thermodynamically favorable reactions by microbes, have important influences on CH<sub>4</sub> and N<sub>2</sub>O emissions (Ardón et al., 2013; Egger et al., 2014; Schoepfer et al., 2014). Additionally, salinity has been reported to alter the availability of substrates (Craft, 2007; Ardón et al., 2013; Morrissey et al., 2014; Schoepfer et al., 2014) and microbial pathways in estuarine and intertidal wetlands

(Crump et al., 2004; Morrissey et al., 2014). Therefore, the changes induced by salinity can drive a series of interrelated biotic processes (Ardón et al., 2013; Helton et al., 2014; Schoepfer et al., 2014), which likely alter the biogeochemical controls regulating CH<sub>4</sub> and N<sub>2</sub>O emissions in estuarine and intertidal environments.

Currently, the occurrence of saltwater incursion into freshwater wetlands has increased due to climate change and reduced water flow (Dai et al., 2011), which potentially affects microbial structure and biogeochemical cycling in the Yangtze Estuary. Although studies of carbon and nitrogen cycling processes have been carried out recently, the biogeochemical controls on greenhouse gas emissions remain unclear in the intertidal wetlands of the Yangtze Estuary. In this study, we provided biogeochemical evidence for microbial mechanisms of salinity-induced changes in CH<sub>4</sub> and N<sub>2</sub>O emissions from an intertidal wetland of the Yangtze Estuary. The main objective of this study was to reveal the effects of elevated salinity on CH<sub>4</sub> and N<sub>2</sub>O emissions and the associated functional genes. The geochemical properties and extracellular enzyme activities of the sediment were also measured to determine the mechanisms of increasing or reducing CH<sub>4</sub> and N<sub>2</sub>O emissions. This work may provide novel insights into the biogeochemical cycling of carbon and nitrogen induced by salinity changes in estuarine and intertidal environments.

## 2. Experimental design and methods

### 2.1. Site description and sediment sampling

The Yangtze Estuary is located in the center of the east coast of China and is subject to a typical subtropical monsoon climate, with an average annual temperature of 15.3 °C and precipitation of 1100 mm (Tang et al., 2011). The intertidal wetlands of the Yangtze Estuary experience great variability in salinity levels, ranging from annual mean of 0.2 to 17‰. Because the freshwater-dominated wetlands of the Yangtze Estuary are often subjected to saltwater incursion during the dry season and tidal fluctuation, a freshwater wetland was consequently selected as the case-study site. In this work, sediment was collected from the surface layer (0–10 cm depth) of a freshwater site located in Xupu (XP, 0.2‰ salinity), Yangtze Estuary (Fig. S1). In June 2016, the sediment sample was collected, placed in airtight plastic bags and returned to the laboratory on ice. At the lab, the sediment was homogenized and subdivided for analysis of physicochemical properties and incubation experiments treated with salinity gradients. The basic chemical and physical properties of the sediment are provided in Table S1, Supporting Information.

### 2.2. Incubation experiments and CH<sub>4</sub> and N<sub>2</sub>O fluxes measurement

In this study, a pot (20 cm diameter, 20 cm height) made of polypropylene plastic was used for sediment incubation. Water samples with 0, 5, 10, 15, 20 and 25‰ salinity were made of the artificial seawater and prepared for the incubation water. The homogenized sediment was transferred into the pots. These pots were spilt into six treatments with four replicates receiving the different salinity water. Two kg of artificial seawater was mixed with 5 kg of fresh sediment and the sediment was balanced by preincubating for two days in dark conditions. Subsequently, these pots were put in an incubator at a temperature of 25 °C. Distilled water was added when weight loss occurred during the five weeks of incubation.

Five weeks later, the potential fluxes of methane (CH<sub>4</sub>) and nitrous oxide (N<sub>2</sub>O) were determined using a closed chamber. The chamber was made of polypropylene plastic including the base and lid. The base of the cylindrical flux chamber was 30 cm in diameter and 50 cm in height. In addition, lid was also made of polypropylene plastic with the same diameter as the base. When the lid was closed, it compressed a rubber gasket cemented to its underside against a horizontal flange at the top of the base walls, thus providing a gas seal (Xu et al., 2014). The gas sample (20 mL) was sampled at 0 and 5 h after chamber closure to

measure the changes in concentrations of CH<sub>4</sub> and N<sub>2</sub>O. CH<sub>4</sub> and N<sub>2</sub>O concentrations were analyzed with a gas chromatograph (GC-2014, Shimadzu) equipped with a flame ionization detector (FID) and electron capture detector (ECD). The column temperature was set at 50 °C, and the FID and ECD temperatures were set at 200 °C and 250 °C, respectively.

Additionally, the sediment was collected after five weeks of incubation, and then separated into three parts for subsequent analyses. The first fraction was immediately stored at –80 °C for measurement of gene abundances. The second fraction was stored at 4 °C for determination of water content, nitrate, nitrite, ammonium, potential nitrification rate (PNR), denitrification enzyme activity (DEA), extracellular enzyme activity (EEA), microbial biomass carbon (MBC) and nitrogen (MBN) within two days. Finally, the third fraction was freeze-dried for analyses of sediment pH, total organic carbon (TOC), labile organic carbon (LOC), recalcitrant organic carbon (ROC) and total nitrogen (TN).

### 2.3. Measurements of nitrogen transformation processes

In this study, the chlorate inhibition method as described by Xu et al. (2014) was used to determine the potential nitrification rate (PNR). The phosphate buffer solution (PBS) was made of 8.0 g NaCl, 0.2 g KCl, 0.2 g Na<sub>2</sub>HPO<sub>4</sub>, 0.2 g NaH<sub>2</sub>PO<sub>4</sub>, and 0.132 g (NH<sub>4</sub>)<sub>2</sub>SO<sub>4</sub> per liter, and then the solution pH was adjusted to 7.4. Next, 5 g of fresh sediment was mixed with 20 mL of PBS in a 50-mL centrifuge tube. Subsequently, 24.5 mg of potassium chlorate was added to each tube (at a concentration of 10 mmol L<sup>-1</sup>) to inhibit oxidation of nitrite from the nitrification. The mixed solution was adequately homogenized by hand before incubation. Subsequently, the sediment suspension was incubated at the temperature of 25 °C for 24 h. The nitrite in the incubated solution was extracted with 5 mL of 2 mol L<sup>-1</sup> KCl solution and determined by a continuous-flow nutrient autoanalyzer (SAN plus, Skalar Analytical B.V., Breda, The Netherlands).

The denitrification enzyme activity (DEA) was determined using the acetylene (C<sub>2</sub>H<sub>2</sub>) inhibition technique, which is widely used in measuring the denitrification process (Guo et al., 2011). The incubation buffer solution was made of 1 mmol L<sup>-1</sup> glucose and 1 mmol L<sup>-1</sup> KNO<sub>3</sub>. Then, 10 g of fresh sediment was mixed with 10 mL buffer solution in a 100-mL serum bottle. The nottle was flushed with high purity helium for 3–5 min and then sealed. In each bottle, 10 mL of headspace gas was replaced with an equal volume of C<sub>2</sub>H<sub>2</sub>, resulting in a final concentration of 10% (v/v) in the headspace to inhibit the reduction of N<sub>2</sub>O to N<sub>2</sub>. After 5 h incubation, N<sub>2</sub>O concentrations in the headspace were analyzed on a gas chromatograph (GC-2014, Shimadzu) equipped with an electron capture detector. The amount of N<sub>2</sub>O in the headspace and DEA were calculated according to the method described by Guo et al. (2011).

### 2.4. Extracellular enzyme activity and microbial biomass

In this study, the extracellular enzyme activities including the C-cycling (sucrose, SUC, cellulose, CEL), polyphenol oxidase (PPO), N-cycling (urease, URE), alkaline phosphatase (AP) and arylsulfatase (AS) were measured with the slightly modified methods described by Alster et al. (2013), Du et al. (2014) and Li et al. (2015). In brief, 5 g of freeze-dried sediment was mixed with respective substrate at the optimal pH and incubated at 25 °C with sporadic gentle agitation for 24 h. The suspension was centrifuged and transferred into a clean tube. The reagent for the enzyme was added to the suspension solutions for colorimetric analysis. In addition, substrate and sample blanks receiving substrate and deionized water were respectively performed in all assays. The absorbance was measured on a microplate reader (SpectraMax M5 Molecular Devices Corporation, Sunnyvale, CA). The extracellular enzyme activities were calculated based on the linear regression between the standard concentrations gradients and the absorbance.

Microbial biomass in sediment was measured with the chloroform fumigation method. In brief, 5 g of fresh sediment was fumigated with

ethanol-free chloroform at 28 °C for 24 h, and then extracted with 20 mL of 0.5 mol L<sup>-1</sup> K<sub>2</sub>SO<sub>4</sub> solution, shaken for 30 min and then centrifuged at 3000 rpm for 10 min. In addition, 5 g of fresh sediment was directly extracted with 20 mL of 0.5 mol L<sup>-1</sup> K<sub>2</sub>SO<sub>4</sub> solution. These supernatants were filtered and stored in –20 °C until analysis. The dissolved organic carbon (DOC) and nitrogen (DON) in the supernatants were measured using a TOC-V<sub>CPH</sub> analyzer (Shimadzu, Japan) and a continuous flow auto analyzer (SAN plus, Skalar Analytical B.V., the Netherlands), respectively. MBC and MBN were calculated as the differences in the DOC and DON before and after fumigation divided by 0.38 and 0.54, respectively (Vance et al., 1987; Brookes et al., 1985).

### 2.5. Sediment geochemical analysis

Water content was determined by the weight loss of sediments before and after being oven-dried for 72 h at 105 °C. Sediment was mixed with water at a ratio (w/v) of 1:2.5 and the pH was measured using a Mettler-Toledo (Hou et al., 2013). Total organic carbon (TOC) and total nitrogen (TN) in sediments was determined using a thermal combustion furnace analyzer (Elementar analyzer vario MAXCNOHS, Germany) after being leached by 1 mol L<sup>-1</sup> HCl (Hou et al., 2013). Sediment NH<sub>4</sub><sup>+</sup>, NO<sub>3</sub><sup>-</sup> and NO<sub>2</sub><sup>-</sup> were extracted with 2 mol L<sup>-1</sup> KCl solution and then determined using a continuous-flow nutrient autoanalyzer (SAN plus, Skalar Analytical B.V., Breda, The Netherlands) with detection limits of 0.5 μmol L<sup>-1</sup> for NH<sub>4</sub><sup>+</sup> and 0.1 μmol L<sup>-1</sup> for NO<sub>3</sub><sup>-</sup>/NO<sub>2</sub><sup>-</sup> (Hou et al., 2013). Labile organic carbon (LOC) was determined by the KMnO<sub>4</sub> oxidation method (Vieira et al., 2007; Du et al., 2014). Recalcitrant organic carbon (ROC) contents were determined using a thermal combustion furnace analyzer after the sediment was hydrolyzed by HCl (Du et al., 2014).

### 2.6. DNA extraction and qPCR

Total DNA was extracted from 0.25 g of fresh sediment using the Power Soil® Total DNA Isolation Kit (MoBio, USA) according to the accompanying instruction. The copy numbers of bacterial and archaeal 16S rRNA, bacterial and archaeal *amoA*, *mcrA*, *pmoA*, *nirK*, *nirS* and *nosZ* in DNA were determined using the 7500 real-time PCR system (Applied Biosystems, Canada) using the SYBR Green qPCR method (Hales et al., 1996; Holmes et al., 1999; Costello and Lidstrom, 1999; Xu et al., 2014; Hou et al., 2015). The qPCR reaction system was performed in 25 μL of solution including 12.5 μL of Maxima SYBR Green/RoxqPCR Master Mix, 1 μL of each primer (10 μmol L<sup>-1</sup>), 1 μL of DNA and 9.5 μL of ddH<sub>2</sub>O. All reactions were performed in 8-strip thin-well PCR tubes with ultraclean cap strips (ABgene, UK). The plasmid pGEM-T Easy Vector (3015 bp, Promega, Madison, U.S.A.) was used for cloning gene fragments to construct the standard curves of qPCR. The standard curves were constructed according to the serial 10-dilution of the plasmid DNA. Cycling reaction conditions and primers in the qPCR analyses are given in the Supporting Information.

### 2.7. Statistical analysis

All statistical analyses were performed using SPSS version 19.0 for Window (SPSS Inc., Chicago, IL, USA). Genes abundance was transformed with a log(10) for all subsequent statistical analyses. Statistical analyses for comparing the obtained data under the salinity treatments were conducted using a one-way analysis of variance (ANOVA). Pearson correlation analysis was used to describe the relationships among sediment properties, functional gene abundances, CH<sub>4</sub> and N<sub>2</sub>O fluxes, and nitrogen transformation rates. In addition, stepwise multiple regression analysis was conducted to reveal the strongest determinant of CH<sub>4</sub> and N<sub>2</sub>O emission rates.

### 3. Results

#### 3.1. Sediment properties

Sediment biogeochemical characteristics along with the salinity gradients are shown in Table 1. The sediment TOC and ROC contents decreased strongly with the increasing salinity, varying from 8.53 to 8.09 mg g<sup>-1</sup> and from 7.05 to 6.10 mg g<sup>-1</sup>, respectively. However, sediment LOC increased significantly with the increasing salinity, increasing from 1.16 to 1.99 mg g<sup>-1</sup>. Sediment MBC and MBN decreased significantly with the increasing salinity, ranging from 219 to 57 μg g<sup>-1</sup> and from 58.8 to 31.7 μg g<sup>-1</sup>, respectively. Sediment TN decreased while the C/N ratio increased with increasing salinity. NH<sub>4</sub><sup>+</sup> concentrations were significantly higher in the treatments of 0, 5 and 10‰ than in the treatments of 15, 20 and 25‰. Likewise, 25‰ salinity had strong influences on NO<sub>x</sub><sup>-</sup> concentration. Overall, high salinity promoted LOC and NO<sub>x</sub><sup>-</sup> accumulation, NH<sub>4</sub><sup>+</sup> consumption, while decreased microbial biomass.

#### 3.2. Sediment extracellular enzyme activities

The rates of measured enzymes varied significantly along with the salinity treatments (Table 2). For the hydrolytic carbon-degrading enzymes (SUC and CEL), the rates of SUC were significantly lower in the 25‰ treatment than other treatments. CEL also increased with the increasing salinity (0–20‰ treatments). The rates of PPO degrading lignin ranged from 170.6 μmol g<sup>-1</sup> h<sup>-1</sup> at 0‰ treatment to 587.7 μmol g<sup>-1</sup> h<sup>-1</sup> at 20‰ treatment. Low rates of URE were observed in the low salinity treatments (0 and 5‰), and the rates increased with increasing salinity. The activity of AP also varied from the treatment with the lowest activity (0‰ = 0.171 μmol g<sup>-1</sup> h<sup>-1</sup>) to the treatment with the highest activity (20‰ = 0.263 μmol g<sup>-1</sup> h<sup>-1</sup>). In addition, the elevated salinity promoted the activity of AS, ranging from 0.084 to 0.159 μmol g<sup>-1</sup> h<sup>-1</sup>. Overall, elevated salinity generally promoted sediment extracellular enzyme activities.

#### 3.3. CH<sub>4</sub> and N<sub>2</sub>O emission rates

CH<sub>4</sub> emission rates in 10 and 15‰ treatments (2.11 and 2.29 μg m<sup>-2</sup> h<sup>-1</sup>, respectively) were significantly lower than in 20 and 25‰ treatments (3.14 and 3.60 μg m<sup>-2</sup> h<sup>-1</sup>, respectively), and higher than in 0 and 5‰ treatments (1.19 and 1.21 μg m<sup>-2</sup> h<sup>-1</sup>, respectively) (Fig. 1A). The highest CH<sub>4</sub> emission rate (3.60 μg m<sup>-2</sup> h<sup>-1</sup>) was observed at the 25‰ treatment (Fig. 1A), which was 3-fold of 0‰ treatment (1.19 μg m<sup>-2</sup> h<sup>-1</sup>). Increasing salinity significantly promoted N<sub>2</sub>O emission rates, ranging from 13.0 μg m<sup>-2</sup> h<sup>-1</sup> of the 10‰ treatment to 22.36 μg m<sup>-2</sup> h<sup>-1</sup> of the 20‰ treatment (Fig. 1B). N<sub>2</sub>O emission rates in 15‰, 20‰ and 25‰ treatments were higher compared to those of the 0‰, 15‰ and 25‰ treatments. Generally, elevated salinity could significantly accelerate the CH<sub>4</sub> and N<sub>2</sub>O emission rates.

#### 3.4. Nitrification and denitrification rates

Elevated salinity accelerated potential nitrification and denitrification enzyme activity (Fig. 2). Potential nitrification rates varied from

0.042 to 0.288 μg N g<sup>-1</sup> h<sup>-1</sup> with the salinity gradients. Nitrification rates were 6-fold higher in the 25‰ treatment (0.288 μg N g<sup>-1</sup> h<sup>-1</sup>) than in the 0‰ treatment (0.042 μg N g<sup>-1</sup> h<sup>-1</sup>). Denitrification enzyme activities varied from the 0‰ treatment with the lowest activity (0.199 μg N g<sup>-1</sup> h<sup>-1</sup>) to the 25‰ treatment with the highest activity (0.309 μg N g<sup>-1</sup> h<sup>-1</sup>). Interestingly, no significant difference in potential nitrification rate and denitrification enzyme activities was observed between the 0 and 5‰ treatments (*p* > 0.05), among the 10, 15 and 20‰ treatments (*p* > 0.05). Overall, nitrification and denitrification showed similar changes in response to the salinity treatments. The highest nitrification and denitrification activities were recorded in the 25‰ treatment followed by the 10, 15 and 20‰ treatments.

#### 3.5. Copy numbers of 16S rRNA and functional genes

The copy numbers of bacterial community, archaeal community, ammonia-oxidizing archaea, ammonia-oxidizing bacteria, methanogens, methanotrophs and denitrifiers in sediments were determined (Fig. 3). Bacterial abundance decreased while archaeal abundance increased with increasing salinity, which varied from 11.8 × 10<sup>11</sup> to 5.53 × 10<sup>11</sup> copies g<sup>-1</sup> and from 0.62 × 10<sup>8</sup> to 3.63 × 10<sup>8</sup> copies g<sup>-1</sup>, respectively. The archaeal *amoA* gene abundance was significantly higher in the treatment of the 25‰ than in the other treatments. Bacterial *amoA* gene decreased with the increasing salinity. Similarly, *nirS* and *nirK* genes copies increased in response to salinity enhancement. However, *nosZ* decreased significantly with the increasing salinity, varying between 7.7 × 10<sup>7</sup> and 2.5 × 10<sup>7</sup> copies g<sup>-1</sup>. The *pmoA* gene abundance decreased from 7.7 × 10<sup>5</sup> to 3.2 × 10<sup>5</sup> copies g<sup>-1</sup> along with the salinity gradients. The increasing salinity had a positive influence on *mcrA* gene abundance, varying from 2.4 × 10<sup>5</sup> to 7.5 × 10<sup>5</sup> copies g<sup>-1</sup>.

### 4. Discussion

#### 4.1. Changes in biogeochemical controls induced by salinity

Elevated salinity has been reported to alter sediment properties, decreasing TOC, ROC, and NH<sub>4</sub><sup>+</sup>, and increasing pH and LOC (Weston et al., 2011; Ardón et al., 2013; Morrissey et al., 2014). In this study, sediment pH was observed to increase with increasing salinity, varying from 7.61 to 8.30. The reason was that high salinity is enriched with alkaline compounds (ca. chloridion), leading to the increase in sediment pH. It has been reported that sediment pH is tightly correlated with the presence of humic substances (Morrissey et al., 2014). In addition, elevated pH can tend to decrease the humic acid sorption capability (Abate & Masini, 2003), which may in return have led to the increasing pH in this study. Organic matter decomposition in sediment is governed by microbial activity (Morrissey et al., 2014). Salinity has been suggested as a regulator of organic matter decomposition and has been tied to rates of microbial respiration in estuarine and coastal wetlands (Weston et al., 2006; Craft, 2007; Loomis and Craft, 2010; Weston et al., 2011; Morrissey et al., 2014). LOC derives from the decomposition of organic matter, thus the high decomposition of organic matter can lead to more LOC accumulation (Broek et al., 2016). In particular, LOC

**Table 1**  
Chemical properties of sediment under the salinity gradients after five weeks incubation.

Salinity (‰)	pH	TOC (mg g <sup>-1</sup> )	LOC (mg g <sup>-1</sup> )	ROC (mg g <sup>-1</sup> )	MBC (μg g <sup>-1</sup> )	MBN (μg g <sup>-1</sup> )	TN (mg g <sup>-1</sup> )	C/N	NH <sub>4</sub> <sup>+</sup> (μg g <sup>-1</sup> )	NO <sub>x</sub> <sup>-</sup> (μg g <sup>-1</sup> )
0	7.61 ± 0.31	8.53 ± 0.06 <sup>a</sup>	1.16 ± 0.13 <sup>c</sup>	7.05 ± 0.12 <sup>a</sup>	219 ± 16 <sup>a</sup>	58.8 ± 9.1 <sup>a</sup>	0.78 ± 0.02 <sup>a</sup>	10.9 ± 0.32 <sup>c</sup>	3.45 ± 0.40 <sup>a</sup>	0.39 ± 0.04 <sup>a</sup>
5	7.53 ± 0.13	8.44 ± 0.09 <sup>a</sup>	1.16 ± 0.20 <sup>c</sup>	6.99 ± 0.13 <sup>a</sup>	192 ± 7.7 <sup>b</sup>	59.4 ± 4.8 <sup>a</sup>	0.75 ± 0.01 <sup>a</sup>	11.2 ± 0.23 <sup>c</sup>	3.18 ± 0.49 <sup>a</sup>	0.23 ± 0.05 <sup>c</sup>
10	7.86 ± 0.24	8.34 ± 0.05 <sup>b</sup>	1.27 ± 0.21 <sup>c</sup>	6.82 ± 0.08 <sup>a</sup>	131 ± 14 <sup>c</sup>	47.9 ± 4.2 <sup>a</sup>	0.73 ± 0.02 <sup>a</sup>	11.4 ± 0.25 <sup>c</sup>	2.38 ± 0.20 <sup>b</sup>	0.34 ± 0.09 <sup>b</sup>
15	8.10 ± 0.18	8.30 ± 0.04 <sup>b</sup>	1.48 ± 0.11 <sup>b</sup>	6.74 ± 0.08 <sup>b</sup>	82 ± 5.4 <sup>d</sup>	40.1 ± 3.3 <sup>ab</sup>	0.61 ± 0.02 <sup>b</sup>	13.7 ± 0.55 <sup>b</sup>	1.01 ± 0.40 <sup>c</sup>	0.59 ± 0.08 <sup>a</sup>
20	8.16 ± 0.28	8.19 ± 0.04 <sup>c</sup>	1.77 ± 0.10 <sup>a</sup>	6.50 ± 0.03 <sup>bc</sup>	70 ± 8.0 <sup>d</sup>	32.4 ± 4.1 <sup>c</sup>	0.52 ± 0.03 <sup>c</sup>	15.8 ± 0.83 <sup>a</sup>	1.36 ± 0.34 <sup>c</sup>	0.37 ± 0.10 <sup>b</sup>
25	8.30 ± 0.12	8.09 ± 0.02 <sup>c</sup>	1.99 ± 0.23 <sup>a</sup>	6.10 ± 0.19 <sup>d</sup>	57 ± 5.8 <sup>de</sup>	31.7 ± 4.9 <sup>c</sup>	0.54 ± 0.04 <sup>c</sup>	15.2 ± 0.99 <sup>a</sup>	1.23 ± 0.31 <sup>c</sup>	0.09 ± 0.03 <sup>d</sup>

Mean ± SD, different letters indicate significant difference between the treatments at *p* < 0.05. NO<sub>x</sub><sup>-</sup>, NO<sub>3</sub><sup>-</sup> plus NO<sub>2</sub><sup>-</sup>.

**Table 2**  
Sediment enzymatic activities under the salinity gradients after five weeks incubation.

Salinity (%)	SUC ( $\mu\text{g g}^{-1} \text{h}^{-1}$ )	CEL ( $\mu\text{g g}^{-1} \text{h}^{-1}$ )	PPO ( $\mu\text{g g}^{-1} \text{h}^{-1}$ )	URE ( $\mu\text{g g}^{-1} \text{h}^{-1}$ )	AP ( $\mu\text{g g}^{-1} \text{h}^{-1}$ )	AS ( $\mu\text{g g}^{-1} \text{h}^{-1}$ )
0	94 $\pm$ 6.8 <sup>c</sup>	2.83 $\pm$ 0.51 <sup>c</sup>	13.3 $\pm$ 1.8 <sup>cd</sup>	0.41 $\pm$ 0.06 <sup>c</sup>	16.0 $\pm$ 0.4 <sup>d</sup>	11.6 $\pm$ 0.9 <sup>d</sup>
5	96 $\pm$ 5.6 <sup>c</sup>	4.38 $\pm$ 0.52 <sup>b</sup>	16.5 $\pm$ 0.8 <sup>c</sup>	0.51 $\pm$ 0.03 <sup>c</sup>	16.9 $\pm$ 0.8 <sup>d</sup>	14.4 $\pm$ 1.1 <sup>c</sup>
10	88 $\pm$ 3.4 <sup>b</sup>	5.67 $\pm$ 0.60 <sup>b</sup>	20.4 $\pm$ 1.8 <sup>b</sup>	0.90 $\pm$ 0.13 <sup>b</sup>	20.6 $\pm$ 0.7 <sup>c</sup>	17.9 $\pm$ 0.7 <sup>b</sup>
15	97 $\pm$ 3.3 <sup>bc</sup>	8.77 $\pm$ 0.60 <sup>a</sup>	27.6 $\pm$ 1.9 <sup>a</sup>	0.57 $\pm$ 0.06 <sup>bc</sup>	22.5 $\pm$ 0.6 <sup>b</sup>	22.1 $\pm$ 1.2 <sup>a</sup>
20	91 $\pm$ 4.5 <sup>a</sup>	10.1 $\pm$ 1.3 <sup>a</sup>	15.2 $\pm$ 1.6 <sup>c</sup>	1.38 $\pm$ 0.07 <sup>a</sup>	24.7 $\pm$ 0.7 <sup>a</sup>	18.6 $\pm$ 0.6 <sup>b</sup>
25	85 $\pm$ 3.6 <sup>b</sup>	5.67 $\pm$ 0.60 <sup>b</sup>	10.9 $\pm$ 1.2 <sup>d</sup>	0.77 $\pm$ 0.13 <sup>b</sup>	17.1 $\pm$ 0.3 <sup>d</sup>	15.5 $\pm$ 1.4 <sup>c</sup>

Mean  $\pm$  SD, different letters indicate significant difference between the treatments at  $p < 0.05$ . SUC, CEL, PPO, URE, AP, and AS are abbreviations for sucrose, cellulose, polyphenol oxidase, urease, alkaline phosphatase and arylsulfatase, respectively.

is the available substrate for microbial activity (Wang et al., 2012), and more LOC provides positive feedback for organic matter decomposition as the result of increasing microbial activity. Thus, the sediment LOC in the present study increased while TOC decreased along with the increasing gradients (Table 1). The ROC, as the main component of TOC, is a poorly decomposable C fraction mainly composed by the lignin and polyphenols (Six et al., 2002). However, in our study, the ROC contents declined likely because the ROC decomposition was stimulated by the increasing salinity (Du et al., 2014). These results show that elevated salinity can stimulate the decomposition of organic matter and is thus favorable for the LOC accumulation.

Microbial biomass has been reported to decrease in response to the increasing salinity (Yan and Marschner, 2012; Q. Zhao et al., 2018). However, some study suggested that the salinity (< 6‰) has no significant influence on microbial biomass (Baldwin et al., 2006). In our study, the microbial biomass carbon in sediment decreased along with the increasing salinity gradients, which is likely because excessively high salinity may stress to microbial metabolism (Hopfensperger et al., 2014). The TN decreased along with the salinity gradients, resulting in the increasing C/N ratios, varying from 10.9 to 15.2 in this study. It has been documented that elevated salinity can also export nitrogen from coastal wetlands to the atmosphere through the exchange of salt cations with sediment  $\text{NH}_4^+$  in coastal wetlands (Ardón et al., 2013). In addition, nitrification and denitrification are sensitive to salinity changes, and salinity can thus accelerate nitrification and denitrification activities through stimulating enzymatic activity (Weston et al., 2011; Morrissey et al., 2014). In this study, the potential nitrification rates were observed to

increase significantly along with the salinity gradients particularly in the 25‰ treatment (Fig. 2). Therefore, the contents of  $\text{NH}_4^+$  in sediments varied significantly along with the salinity gradients, decreasing from low to high salinity treatments (Table 1). In addition, the lowest content of  $\text{NO}_x^-$  in the 25‰ salinity treatment may be attributed to the highest denitrification enzyme activity (Fig. 2) because denitrification contributes most significantly to the nitrate loss in estuarine sediments (Hou et al., 2013).

Salinity affects sediment properties, which may in return lead to the alterations of enzyme activities, microbial communities and functional genes (Morrissey et al., 2014). Increasing salinity led to the decrease in the bacterial 16S rRNA abundance particularly in the 25‰ treatment because excessively high salinity inhibits microbial activity. However, archaeal 16S rRNA was favored by the high salinity relative to the bacterial community, the copy number of archaeal 16S rRNA generally increases from estuarine to marine environments (Hugoni et al., 2015). The bacterial *amoA* gene of nitrification community decreased while archaeal *amoA* gene increased with the increasing salinity, indicating a different response to salinity impact between archaeal and bacterial *amoA* gene. Likewise, Wang et al. (2018) have reported that archaeal *amoA* gene abundance was higher in high salinity than in low salinity, while the bacterial *amoA* gene was higher in intermediate salinity than in high salinity, further suggesting that salinity had different effects on nitrifying communities. In this study, the denitrifier community varied along with the salinity gradients, of which *nirS* and *nirK* increased while *nosZ* decreased with increasing salinity (Fig. 3). Mosier and Francis (2010) reported that a significant correlation was observed

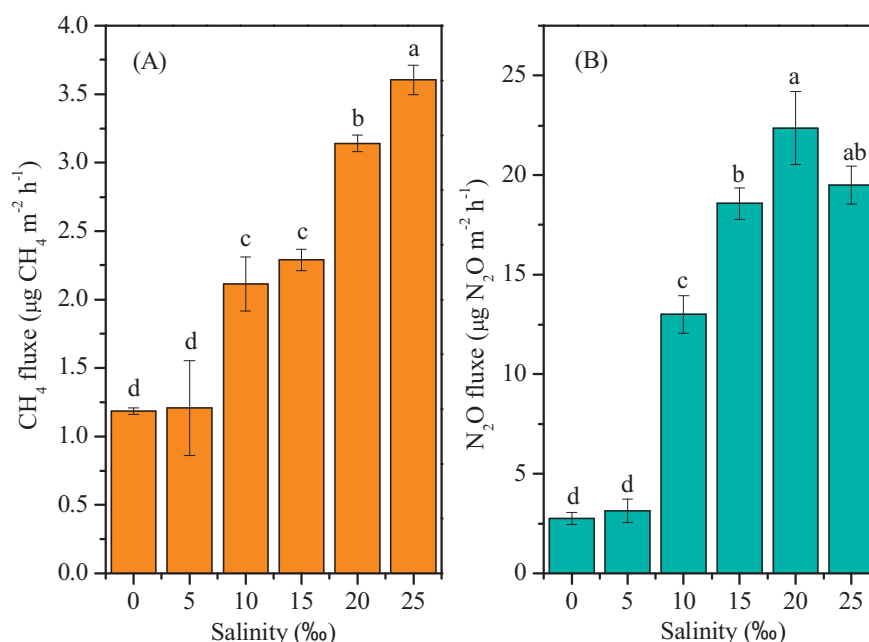


**Fig. 1.**  $\text{CH}_4$  and  $\text{N}_2\text{O}$  emission rates in the sediment after five weeks incubation under the salinity gradients stress. Error bars represent standard errors ( $n = 4$ ).

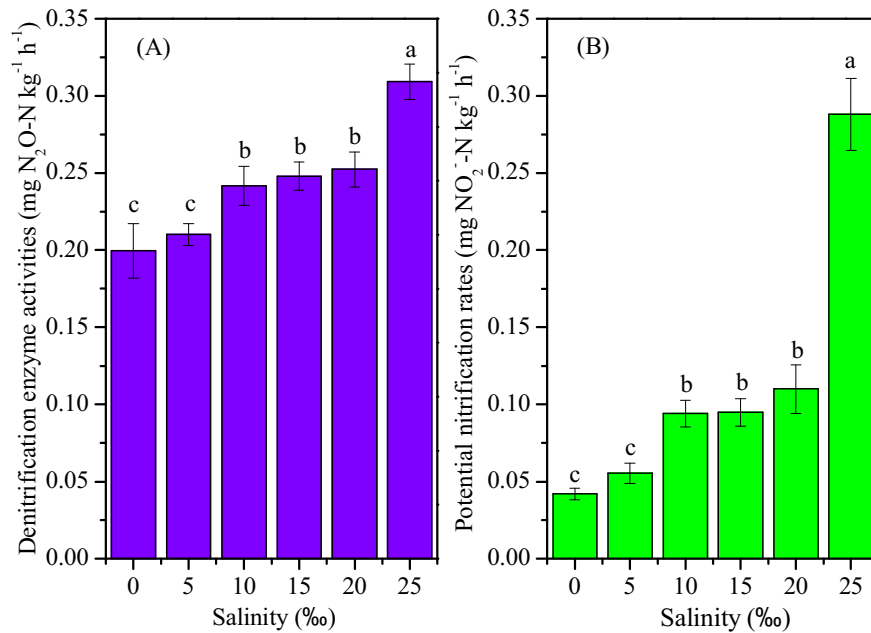


**Fig. 2.** Denitrification enzyme activities (A) and potential nitrification rates (B) of the sediment under the salinity gradients. The different small letters above the column denote statistically significant differences between the salinity gradients ( $p < 0.05$ ). Error bars represent standard errors ( $n = 4$ ).

between salinity and abundances of *nirK* and *nirS* genes in the San Francisco Bay estuary, indicating that intermediate salinity is favorable for the *nirK* and *nirS* of the denitrifying community. In addition, it has been reported that the *nosZ* gene is significantly lower in high salinity than in low salinity (Wang et al., 2018). It has been reported that *mcrA* gene abundance is higher in freshwater marshes than in brackish marshes, indicating that salinity is still a major factor controlling

methanogens in the low level salinity gradients of estuarine environments (Tong et al., 2017). Shen et al. (2014) reported that the *pmoA* gene abundance was lower in high salinity than in low salinity sites. However, in our study, the functional *pmoA* gene of methanotrophs decreased with the increasing salinity, while the *mcrA* gene of methanogens increased in response to the increasing salinity likely because the sediment variables differed in incubation experiment

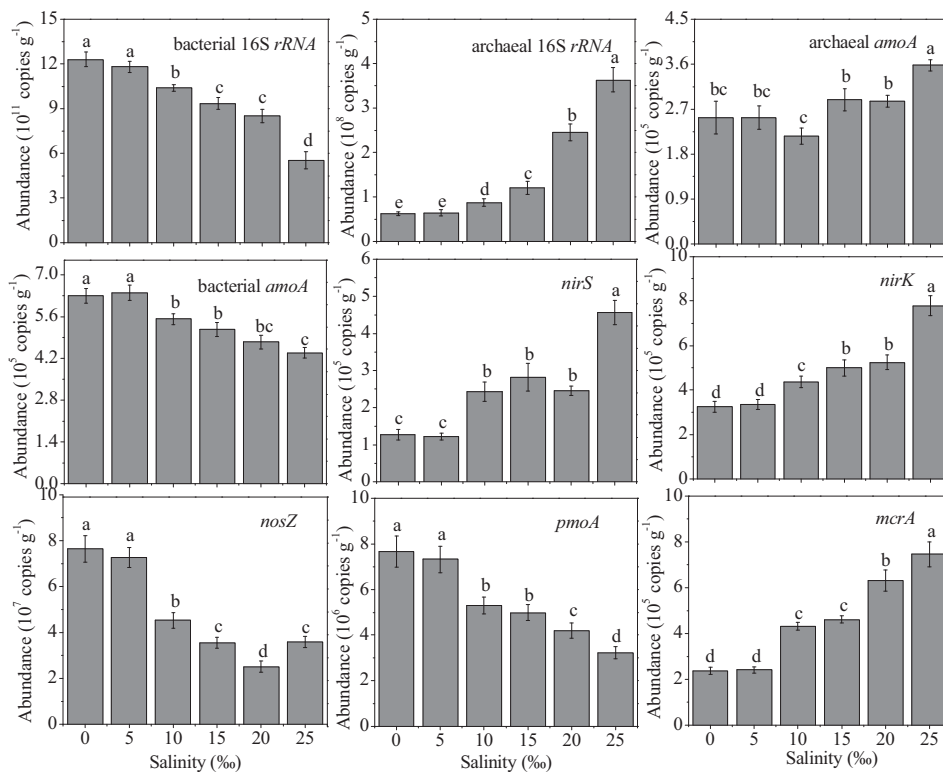


**Fig. 3.** Copy numbers of archaeal and bacterial 16S rRNA, archaeal and bacterial *amoA*, *nirK*, *nirS*, *nosZ*, *mcrA* and *pmoA* genes in the sediments under the salinity gradients. Significant differences among the salinity gradients are indicated by different letters ( $p < 0.05$ ).

compared to the field environments. In addition, the sediment enzyme activities were generally enhanced by the increasing salinity, because salinity can improve the bioavailability of organic substrates and thus facilitates enzymatic activity at a modest level of salinity (Neubauer et al., 2013; Morrissey et al., 2014). However, many studies have suggested that hypersaline conditions inhibit enzyme activity, because excessively high salinity has negative influence on molecular stability and protein conformational states (Yun et al., 2010; Pan et al., 2013). Therefore, the sediment enzyme activities increased with the increasing salinity (0–20‰), which further supported the reported correlation between the salinity and enzyme activity. Overall, these results demonstrate that salinity may alter not only sediment characteristics but also microbial community abundance by mediating the substrates for microbial communities (Baldwin et al., 2006; Weston et al., 2011; Neubauer et al., 2013; Morrissey et al., 2014).

#### 4.2. Effects of biogeochemical properties on CH<sub>4</sub> and N<sub>2</sub>O emissions

Salinity was observed to influence CH<sub>4</sub> and N<sub>2</sub>O emissions through indirectly and directly affecting sediment properties and microbial communities (Poffenbarger et al., 2011; Murray et al., 2015). Anaerobic decomposition of organic matter can produce CH<sub>4</sub>, which contributes to the main parts of CH<sub>4</sub> generation in the sediment (Avery et al., 2003). Thus, organic carbon may be a strong determinant of the CH<sub>4</sub> emission rate in the sediment. In this study, the LOC and C/N showed significantly positive correlations with CH<sub>4</sub> emission rates ( $p < 0.01$ ), indicating the importance of organic carbon in CH<sub>4</sub> emissions. The CH<sub>4</sub> emission rate was significantly related to pH, indirectly suggesting that pH was also an important factor regulating CH<sub>4</sub>, because the methanogen activity is favored by alkalinescence (Tong et al., 2017). Because enzyme activity is the putative rate-limiting step in organic matter decomposition (Morrissey et al., 2014), the enhanced enzymatic activities induced by the increasing salinity may affect the CH<sub>4</sub> emission rate. Sucrose and cellulose mainly perform carbon cycling, and thus may influence CH<sub>4</sub> emissions because the anaerobic fermentation of organic matter can produce methane (Vizza et al., 2017). In this study, URE and CEL showed positive effects on CH<sub>4</sub> emission rates, while SUC had a negative influence on CH<sub>4</sub>. In addition, although the CH<sub>4</sub> oxidation coupled to NO<sub>3</sub><sup>-</sup> and NO<sub>2</sub><sup>-</sup> reduction has been proven important in aquatic environments (Luesken et al., 2011; Noröi & Thamdrup, 2014), the content of NO<sub>x</sub><sup>-</sup> did not vary significantly along the increasing salinity gradients, suggesting that NO<sub>x</sub><sup>-</sup> may not be responsible for CH<sub>4</sub> emission. In our study, stepwise multiple regression analysis suggested that the LOC, pH and SUC were the main factors regulating CH<sub>4</sub> emission, of which LOC was the most important determinant, accounting for 80.5% of the total variation (Fig. 4). LOC is the most available substrate for microbial activity (Morrissey et al., 2014), which can supply abundant energy for the microbial community because most microorganisms are heterotrophic. Methanogens are also heterotrophic microorganisms that require an energy supply in the methane production (Vizza et al., 2017). Thus, the LOC was the most important factor affecting CH<sub>4</sub> emissions.

In this study, LOC and C/N showed significant correlations with N<sub>2</sub>O emission rates ( $p < 0.01$ , Table 3). Previous study has reported that denitrification is favorable to occur in the high availability of organic matter (Plummer et al., 2015), because the denitrifier communities are heterotrophic microorganisms. In addition, denitrification contributes to the largest amount of N<sub>2</sub>O emissions in estuarine environments (Ardón et al., 2013; Murray et al., 2015). Thus, high N<sub>2</sub>O emissions were generally observed in the conditions of high organic carbon where the denitrification activity occurs strongly. The NH<sub>4</sub><sup>+</sup> also had a great influence on the N<sub>2</sub>O emissions, implying that NH<sub>4</sub><sup>+</sup> was an important factor in N<sub>2</sub>O emission. Generally, NH<sub>4</sub><sup>+</sup> oxidation into NO<sub>3</sub><sup>-</sup> can supply abundant substrate for denitrification because NO<sub>3</sub><sup>-</sup> is limited in the environment (Russow et al., 2009). In our study, the relatively lower contents of NH<sub>4</sub><sup>+</sup> in high salinity treatments were observed compared to low salinity treatments, which indicated that the high

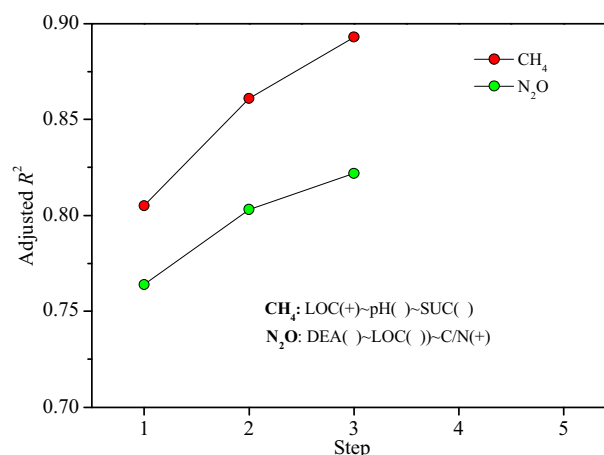


**Fig. 4.** Stepwise multiple regression analysis between CH<sub>4</sub> and N<sub>2</sub>O with the sediment variables. The data has been transformed normally before entered into the models. For each model, final set of predictors is shown in sequence. '+' and '-' in the brackets denote positive and negative relationships between CH<sub>4</sub> and N<sub>2</sub>O and predictors, respectively.

nitrification rates may contribute to the increasing N<sub>2</sub>O emissions in the high salinity treatments because the aerobic NH<sub>4</sub><sup>+</sup> oxidation can also produce N<sub>2</sub>O (Murray et al., 2015). In addition, the URE was observed to have a significant correlation with N<sub>2</sub>O emission rate. It has been reported that URE is the most important enzyme in nitrogen cycling, and can catalyze urea into NH<sub>4</sub><sup>+</sup> (Pan et al., 2013), thus further supplying the substrate for the nitrification process. The Fe(II) level can be enhanced by the increasing salinity (Baldwin et al., 2006), which may result in an increasing denitrification capacity because the Fe(II)-driven nitrate reduction is involved in denitrification (called

**Table 3**

Pearson correlation between CH<sub>4</sub> and N<sub>2</sub>O emission rates and biogeochemical controls ( $n = 24$ ).

Biogeochemical controls	CH <sub>4</sub>		N <sub>2</sub> O	
	<i>r</i>	<i>p</i>	<i>r</i>	<i>p</i>
<b>Abiotic factor</b>				
Salinity				
pH	0.88	0.00	-0.76	0.00
LOC	0.84	0.00	0.72	0.00
MBC	-0.87	0.00	-0.94	0.00
MBN	-0.86	0.00	-0.88	0.00
ROC	-0.88	0.00	-0.71	0.00
LOC/ROC	0.85	0.00	0.70	0.00
TOC	-0.90	0.0	-0.83	0.00
TN	-0.89	0.00	-0.80	0.00
C/N	0.86	0.00	0.81	0.00
NH <sub>4</sub> <sup>+</sup>	-0.77	0.00	-0.88	0.00
NO <sub>3</sub> <sup>-</sup>	-0.31	0.14	-0.06	0.79
<b>Biotic factor</b>				
URE	0.60	0.002	0.66	0.00
SUC	-0.55	0.006	-0.30	0.16
CEL	0.56	0.004	0.76	0.00
PPO	-0.17	0.44	0.20	0.36
AP	0.40	0.05	0.67	0.00
AS	0.38	0.07	0.71	0.00
PNR	0.79	0.00	0.60	0.002
DEA	0.85	0.00	0.77	0.00
<b>Genes abundance</b>				
Archaeal <i>amoA</i>	0.68	0.00	0.55	0.00
Bacterial <i>amoA</i>	-0.93	0.00	-0.89	0.00
<i>nirS</i>	0.88	0.00	0.85	0.00
<i>nirK</i>	0.91	0.00	0.83	0.00
<i>nosZ</i>	-0.83	0.00	-0.94	0.00
<i>mcrA</i>	0.93	0.00	0.92	0.00
<i>pmoA</i>	-0.94	0.00	-0.88	0.00

chemodenitrification) (Jones et al., 2015). Further study regarding the underlying interaction between Fe(II) and denitrification is thus required. In our study, salinity had a great influence on nitrification, and nitrification may thus partially contribute to increasing N<sub>2</sub>O emissions because nitrification can also produce N<sub>2</sub>O during the NH<sub>4</sub><sup>+</sup> oxidation (Hu et al., 2012). Therefore, in our study, the stepwise regression analysis suggested that denitrification dominated the N<sub>2</sub>O emission rates followed by LOC, accounting for 76.4% and 3.9% of their total variations, respectively (Fig. 4). Both denitrification and LOC were observed to increase with the salinity gradients (Fig. 1, Table 1). In addition, denitrification was affected by the LOC, while N<sub>2</sub>O production was mainly controlled by the denitrification. Thus, it was noted that denitrification not LOC dominated the N<sub>2</sub>O emissions in this study, highlighting the importance of denitrification in N<sub>2</sub>O emissions.

In addition to affecting sediment properties, the changes in CH<sub>4</sub> and N<sub>2</sub>O emission rates could also be attributed to the differences in microbial diversity and abundance induced by salinity (Henry et al., 2006; Q. Zhao et al., 2018). Elevated salinity could lead to the decreases in bacterial abundance but increases in archaeal abundance, supporting the observation of reduced microbial biomass induced by the increasing salinity, as bacterial abundance dominates the total microbial community in the sediment (S.Y. Zhao et al., 2018). Elevated salinity increased the activities of nitrification and denitrification, suggesting that denitrification and nitrification are sensitive to the salinity (Wang et al., 2018). The archaeal *amoA* gene may contribute more than bacterial *amoA* to the enhanced nitrification, because the archaeal *amoA* gene abundance was strongly increased by the elevated salinity, but bacterial *amoA* (Fig. 3). Previous research has also suggested that salinity can accelerate nitrification, and the archaeal *amoA* gene abundance could better explain the nitrification dynamics relative to bacterial *amoA* (Zheng et al., 2014).

Although the denitrification activity was stimulated by the increasing salinity (Fig. 2), the *nirS*, *nirK* and *nosZ* of denitrifier communities varied along with the salinity gradients (Fig. 3). Previous studies have reported that *nirS* and *nirK* are the microbial producers of N<sub>2</sub>O, while *nosZ* reduces N<sub>2</sub>O to N<sub>2</sub> (Henry et al., 2006; S.Y. Zhao et al., 2018), indicating that denitrifier communities are the crucial factors affecting the N<sub>2</sub>O emission. In this study, the copy numbers of *nirS* and *nirK* genes increased while those of *nosZ* gene decreased along with the salinity gradients. Thus, the changes in *nirS* and *nirK* gene abundances could account for the differences in N<sub>2</sub>O emission rates along with the salinity gradients. In addition, the maximum N<sub>2</sub>O emission rate in the 25‰ treatment was observed, which was supported by that the copy numbers of *nirS* and *nirK* genes were significantly higher in 25‰ treatment than in other salinity treatments. Therefore, the N<sub>2</sub>O emission was mainly controlled by *nirS* and/or *nirK* in this study. In addition, the abundance of *mcrA* gene was significantly related to CH<sub>4</sub> emission rates (Table 3), indicating that the methanogens activity has an important influence on CH<sub>4</sub> emission. Likewise, it has also been suggested that the enhanced copy number of *mcrA* gene can lead to the increasing CH<sub>4</sub> emission by methanogen producers (Tong et al., 2017). In addition, the decreased abundance of *pmoA* gene may mitigate the methane oxidation, which also may contribute to the enhanced CH<sub>4</sub> emission rates in high salinity treatments.

In summary, elevated salinity was found to accelerate CH<sub>4</sub> and N<sub>2</sub>O emissions by changing sediment characteristics and stimulating the microbial enzyme activities. Additionally, salinity was observed to increase the abundances of the functional genes *mcrA*, *nirS* and *nirK*, which were likely the biotic factors mediating the enhanced CH<sub>4</sub> and N<sub>2</sub>O emission rates. In contrast, elevated salinity enhanced carbon and nitrogen export by stimulating organic matter decomposition and nitrogen transformation processes, thus decreasing the carbon sequestration and nitrogen retention in estuarine environments. Overall, the importance of salinity in CH<sub>4</sub> and N<sub>2</sub>O emissions should be attracted attention particularly where estuarine and intertidal ecosystems are widely influenced by saltwater incursion under climate change.

## Acknowledgments

This work was supported by the National Natural Science Foundation of China (Grant Nos. 41701548, 41761144062 and 41671463), the Foundation for Excellent Youth Scholar of Fujian Normal University.

## Appendix A. Supplementary data

Supplementary data to this article can be found online at <https://doi.org/10.1016/j.scitotenv.2018.10.294>.

## References

- Abate, G., Masini, J.C., 2003. Influence of pH and ionic strength on removal processes of a sedimentary humic acid in a suspension of vermiculite. *Colloids Surf. A Physicochem. Eng. Asp.* 226, 25–34.
- Alster, C.J., German, D.P., Lu, Y., Allison, S.D., 2013. Microbial enzymatic responses to drought and to nitrogen addition in a southern California grassland. *Soil Biol. Biochem.* 64, 68–79.
- Ardón, M., Morse, J.L., Colman, B.P., Bernhardt, E.S., 2013. Drought-induced saltwater incursion leads to increased wetland nitrogen export. *Glob. Chang. Biol.* 19 (10), 2976–2985.
- Avery, G.B., Shannon, R.D., White, J.R., Martens, C.S., Alperin, M.J., 2003. Controls on methane production in a tidal freshwater estuary and a peatland: methane production via acetate fermentation and CO<sub>2</sub> reduction. *Biogeochemistry* 62 (1), 19–37.
- Baldwin, D.S., Rees, G.N., Mitchell, A.M., Watson, G., Williams, J., 2006. The short-term effects of salinization on anaerobic nutrient cycling and microbial community structure in sediment from a freshwater wetland. *Wetlands* 26 (2), 455–464.
- Bastviken, D., Tranvik, L.J., Downing, J.A., Crill, P.M., Enrich-Prast, A., 2011. Freshwater methane emissions offset the continental carbon sink. *Science* 331 (6013), 50.
- Broek, M.V.D., Temmerman, S., Merckx, R., Govers, G., 2016. Controls on soil organic carbon stocks in tidal marshes along an estuarine salinity gradient. *Biogeosciences* 13 (24), 6611–6624.
- Brookes, P.C., Landman, A., Pruden, G., Jenkinson, D.S., 1985. Chloroform fumigation and the release of soil nitrogen: a rapid direct extraction method to measure microbial biomass nitrogen in soil. *Soil Biol. Biochem.* 17, 837–842.
- Church, J.A., White, N.J., 2006. A 20th century acceleration in global sea-level rise. *Geophys. Res. Lett.* 33, L01602.
- Costello, A.M., Lidstrom, M.E., 1999. Molecular characterization of functional and phylogenetic genes from natural populations of methanotrophs in lake sediments. *Appl. Environ. Microbiol.* 65, 5066–5074.
- Craft, C., 2007. Freshwater input structures soil properties, vertical accretion, and nutrient accumulation of Georgia and US tidal marshes. *Limnol. Oceanogr.* 52, 1220–1230.
- Crump, B.C., Hopkinson, C.S., Sogin, M.L., Hobbie, J.E., 2004. Microbial biogeography along an estuarine salinity gradient: combined influences of bacterial growth and residence time. *Appl. Environ. Microbiol.* 70, 1494–1505.
- Dai, Z.J., Chu, A., Stive, M., Zhang, X.L., Yan, H., 2011. Unusual salinity conditions in the Yangtze estuary in 2006: impacts of an extreme drought or of the Three Gorges Dam? *Ambio* 40 (5), 496–505.
- Deng, F.Y., Hou, L.J., Liu, M., Zheng, Y.L., Yin, G.Y., Li, X.F., Lin, X.B., Chen, F., Gao, J., Jiang, X.F., 2015. Dissimilatory nitrate reduction processes and associated contribution to nitrogen removal in sediments of the Yangtze estuary. *J. Geophys. Res. Biogeosci.* 120 (8), 1521–1531.
- Du, Y.H., Guo, P., Liu, J.Q., Wang, C.Y., Yang, N., Jiao, Z.X., 2014. Different types of nitrogen deposition show variable effects on the soil carbon cycle process of temperate forests. *Glob. Chang. Biol.* 20 (10), 3222–3228.
- Egger, M., Rasigraf, O., Sapart, C.J., Jilbert, T., Jetten, M.S.M., Röckmann, T., van der Veer, C., Bändä, N., Kartal, B., Ettwig, K.F., Slomp, C.P., 2014. Iron-mediated anaerobic oxidation of methane in Brackish coastal sediments. *Environ. Sci. Technol.* 49 (1), 277–283.
- Franklin, R.B., Morrissey, E.M., Morina, J.C., 2017. Changes in abundance and community structure of nitrate-reducing bacteria along a salinity gradient in tidal wetlands. *Pedobiologia* 60, 21–26.
- Guo, G.X., Deng, H., Qiao, M., Mu, Y.J., Zhu, Y.G., 2011. Effect of pyrene on denitrification activity and abundance and composition of denitrifying community in an agricultural soil. *Environ. Pollut.* 159 (7), 1886–1895.
- Hales, B.A., Edwards, C., Ritchie, D.A., Hall, G., Pickup, R.W., Saunderson, J.R., 1996. Isolation and identification of methanogen-specific DNA from blanket bog peat by PCR amplification and sequence analysis. *Appl. Environ. Microbiol.* 62 (2), 668–675.
- Harley, J.F., Carvalho, L., Dudley, B., Heal, K.V., Rees, R.M., Skiba, U., 2015. Spatial and seasonal fluxes of the greenhouse gases N<sub>2</sub>O, CO<sub>2</sub> and CH<sub>4</sub> in a UK macrotidal estuary. *Estuar. Coast. Shelf Sci.* 153, 62–73.
- Helton, A.M., Bernhardt, E.S., Fedders, A., 2014. Biogeochemical regime shifts in coastal landscapes: the contrasting effects of saltwater incursion and agricultural pollution on greenhouse gas emissions from a freshwater wetland. *Biogeochemistry* 120 (1–3), 133–147.
- Henry, S., Bru, D., Stres, B., Hallet, S., Philippot, L., 2006. Quantitative detection of the *nosZ* gene, encoding nitrous oxide reductase, and comparison of the abundances of 16S rRNA, *narG*, *nirK*, and *nosZ* genes in soils. *Appl. Environ. Microbiol.* 72, 5181–5189.
- Holmes, A.J., Roslev, P., McDonald, I.R., Iversen, N., Henriksen, K., Murrell, J.C., 1999. Characterization of methanotrophic bacterial populations in soils showing atmospheric methane uptake. *Appl. Environ. Microbiol.* 65, 3312–3318.

- Hopfensperger, K.N., Burgin, A.J., Schoepfer, V.A., Helton, A.M., 2014. Impacts of saltwater incursion on plant communities, anaerobic microbial metabolism, and resulting relationships in a restored freshwater wetland. *Ecosystems* 17 (5), 792–807.
- Hou, L.J., Zheng, Y.L., Liu, M., Gong, J., Zhang, X.L., Yin, G.Y., You, L.L., 2013. Anaerobic ammonium oxidation (anammox) bacterial diversity, abundance, and activity in marsh sediments of the Yangtze estuary. *J. Geophys. Res. Biogeosci.* 118, 1237–1246.
- Hou, L.J., Yin, G.Y., Liu, M., Zhou, J.L., Zheng, Y.L., Gao, J., Zong, H.B., Yang, Y., Gao, L., Tong, C.F., 2015. Effects of sulfamethazine on denitrification and the associated N<sub>2</sub>O release in estuarine and coastal sediments. *Environ. Sci. Technol.* 49, 326–333.
- Hu, Z., Lee, J.W., Chandran, K., Kim, S., Khanal, S.K., 2012. Nitrous oxide (N<sub>2</sub>O) emission from aquaculture: a review. *Environ. Sci. Technol.* 46 (12), 6470–6480.
- Hugoni, M., Agogue, H., Taib, N., Domaizon, I., Moné, A., Galand, P.E., Bronner, G., Debroas, D., Mary, I., 2015. Temporal dynamics of active prokaryotic nitrifiers and archaeal communities from river to sea. *Microb. Ecol.* 70 (2), 473–483.
- IPCC, 2014. Summary for policymakers. *Climate Change 2014: Impacts, Adaptation, and Vulnerability. Part A: Global and Sectoral Aspects. Contribution of Working Group II to the Fifth Assessment Report of the Intergovernmental Panel on Climate Change.* Cambridge University Press, Cambridge, United Kingdom and New York, NY, USA, pp. 1–32.
- Jones, L.C., Peters, B., Lpez Pacheco, J.S., Casciotti, K.L., Fendorf, S., 2015. Stable isotopes and iron oxide mineral products as markers of chemodenitrification. *Environ. Sci. Technol.* 49 (6), 3444–3452.
- Li, X.F., Hou, L.J., Liu, M., Lin, X.B., Li, Y., Li, S.W., 2015. Primary effects of extracellular enzyme activity and microbial community on carbon and nitrogen mineralization in estuarine and tidal wetlands. *Appl. Microbiol. Biotechnol.* 99, 2895–2909.
- Loomis, M.J., Craft, C.B., 2010. Carbon sequestration and nutrient (nitrogen, phosphorus) accumulation in river-dominated tidal marshes, Georgia, USA. *Soil Sci. Soc. Am. J.* 74, 1028–1036.
- Luesken, F.A., Sánchez, J., Van, T.A., Danabria, J., Op den Camp, H.J.M., Jetten, M.S.M., Kartal, B., 2011. Simultaneous nitrite-dependent anaerobic methane and ammonium oxidation processes. *Appl. Environ. Microbiol.* 77, 6802–6907.
- Mandel, Q.A., 2006. Biodiversity of the genus *Fusarium* in saline soil habitats. *J. Basic Microbiol.* 46, 480–494.
- Morrissey, E.M., Gillespie, J.L., Morina, J.C., Franklin, R.B., 2014. Salinity affects microbial activity and soil organic matter content in tidal wetlands. *Glob. Chang. Biol.* 20, 1351–1362.
- Mosier, A.C., Francis, C.A., 2010. Denitrifier abundance and activity across the San Francisco Bay estuary. *Environ. Microbiol. Rep.* 2, 667–676.
- Murray, R.H., Erler, D.V., Eyre, B.D., 2015. Nitrous oxide fluxes in estuarine environments: response to global change. *Glob. Chang. Biol.* 21 (9), 3219–3245.
- Neubauer, S.C., Franklin, R.B., Berrier, D.J., 2013. Saltwater intrusion into tidal freshwater marshes alters the biogeochemical processing of organic carbon. *Biogeosciences* 10, 10685–10720.
- Nordl, K., Thamdrup, B., 2014. Nitrate-dependent anaerobic methane oxidation in a freshwater sediment. *Geochim. Cosmochim. Acta* 132, 141–150.
- Pan, C.C., Liu, C.G., Zhao, H.L., Wang, Y., 2013. Changes of soil physico-chemical properties and enzyme activities in relation to grassland salinization. *Eur. J. Soil Biol.* 55, 13–19.
- Plummer, P., Tobias, C., Cady, D., 2015. Nitrogen reduction pathways in estuarine sediments: influences of organic carbon and sulfide. *J. Geophys. Res.: Biogeosci.* 120 (10), 1958–1972.
- Poffenbarger, H.J., Needelman, B.A., Megonigal, J.P., 2011. Salinity influence on methane emissions from tidal marshes. *Wetlands* 31, 831–842.
- Randeniya, L.K., Vohralik, P.F., Plumb, I.C., 2002. Stratospheric ozone depletion at northern mid latitudes in the 21st century: the importance of future concentrations of greenhouse gases nitrous oxide and methane. *Geophys. Res. Lett.* 29, 101–104.
- Russow, R., Stange, C.F., Neue, H.U., 2009. Role of nitrite and nitric oxide in the processes of nitrification and denitrification in soil: results from <sup>15</sup>N tracer experiments. *Soil Biol. Biochem.* 41 (4), 785–795.
- Schoepfer, V.A., Bernhardt, E.S., Burgin, A.J., 2014. Iron clad wetlands: soil iron-sulfur buffering determines coastal wetland response to salt water incursion. *J. Geophys. Res. Biogeosci.* 119, 2209–2219.
- Shen, L.D., Zhu, Q., Liu, S., Du, P., Zeng, J.N., Cheng, D.Q., Xu, X.Y., Zheng, P., Hu, B.L., 2014. Molecular evidence for nitrite-dependent anaerobic methane-oxidizing bacteria in the Jiaojiang estuary of the East Sea (China). *Appl. Microbiol. Biotechnol.* 98 (11), 5029–5038.
- Six, J., Conant, R.T., Paul, E.A., Paustian, K., 2002. Stabilization mechanisms of soil organic matter: implications for C-saturation of soils. *Plant Soil* 241, 155–176.
- Tang, Y.S., Wang, L., Jia, J.W., Li, Y.L., Zhang, W.Q., Wang, H.L., Sun, Y., 2011. Response of soil microbial respiration of tidal wetlands in the Yangtze River estuary to different artificial disturbances. *Ecol. Eng.* 37, 1638–1646.
- Tong, C., Cadillo-Quiroz, H., Zeng, Z.H., She, C.X., Yang, P., Huang, J.F., 2017. Changes of community structure and abundance of methanogens in soils along a freshwater-brackish water gradient in subtropical estuarine marshes. *Geoderma* 299, 101–110.
- Vance, E.D., Brookes, P.C., Jenkinson, D.S., 1987. An extraction method for measuring soil microbial biomass C. *Soil Biol. Biochem.* 19, 703–707.
- Vieira, F.C.B., Bayer, C., Zanatta, J.A., Dieckow, J., Mielniczuk, J., He, Z.L., 2007. Carbon management index based on physical fractionation of soil organic matter in an Acrisol under long-term no-till cropping systems. *Soil Tillage Res.* 96, 195–204.
- Vizza, C., West, W.E., Jones, S.E., Hart, J.A., Lambert, G.A., 2017. Regulators of coastal wetland methane production and responses to simulated global change. *Biogeosciences* 14 (2), 431–446.
- Wang, H., He, Z.L., Lu, Z.M., Zhou, J.Z., Van Nostrand, J.D., Xu, X.H., Zhang, Z.J., 2012. Genetic linkage of soil carbon pools and microbial functions in subtropical freshwater wetlands in response to experimental warming. *Appl. Environ. Microbiol.* 78, 7652–7661.
- Wang, H.T., Gilbert, J.A., Zhu, Y.G., Yang, X.R., 2018. Salinity is a key factor driving the nitrogen cycling in the mangrove sediment. *Sci. Total Environ.* 631, 1342–1349.
- Weston, N.B., Dixon, R.E., Joye, S.B., 2006. Ramifications of increased salinity in tidal freshwater sediments: geochemistry and microbial pathways of organic matter mineralization. *J. Geophys. Res. Biogeosci.* 111, 2005–2012.
- Weston, N.B., Vile, M.A., Neubauer, S.C., Velinsky, D.J., 2011. Accelerated microbial organic matter mineralization following salt-water intrusion into tidal freshwater marsh soils. *Biogeochemistry* 102, 135–151.
- Wigley, T.M.L., 2005. The climate change commitment. *Science* 307, 1766–1769.
- Xu, H.J., Wang, X.H., Li, H., Yao, H.Y., Su, J.Q., Zhu, Y.C., 2014. Biochar impacts soil microbial community composition and nitrogen cycling in an acidic soil planted with rape. *Environ. Sci. Technol.* 48 (16), 9391–9399.
- Yan, N., Marschner, P., 2012. Response of microbial activity and biomass to increasing salinity depends on the final salinity, not the original salinity. *Soil Biol. Biochem.* 53, 50–55.
- Yun, E.Y., Ro, H.M., Lee, G.T., Choi, W.J., 2010. Salinity effects on chlorophyll degradation and phosphorus fractionation in reclaimed coastal tideland soils. *Geosci. J.* 14, 371–378.
- Zhao, Q., Bai, J.H., Zhang, G., Jia, J., Wang, W., Wang, X., 2018. Effects of water and salinity regulation measures on soil carbon sequestration in coastal wetlands of the Yellow River Delta. *Geoderma* 319, 219–229.
- Zhao, S.Y., Wang, Q., Zhou, J.M., Yuan, D.D., Zhu, G.B., 2018. Linking abundance and community of microbial N<sub>2</sub>O-producers and N<sub>2</sub>O-reducers with enzymatic N<sub>2</sub>O production potential in a riparian zone. *Sci. Total Environ.* 642, 1090–1099.
- Zheng, Y.L., Hou, L.J., Newell, S., Liu, M., Zhou, J.L., Zhao, H., You, L.L., Cheng, X.L., 2014. Community dynamics and activity of ammonia-oxidizing prokaryotes in intertidal sediments of the Yangtze estuary. *Appl. Environ. Microbiol.* 80 (1), 408–419.